JKAS
Journal of the Korean Astronomical Society
http://jkas.kas.org
eISSN: 2288-890X · pISSN: 1225-4614
JKAS (2023), **56**, 1, 35–40
doi: 10.5303/JKAS.2023.56.1.35

A Search for Exoplanets around Northern Circumpolar Stars. VII. Detection of Planetary Companion Orbiting the Largest Host Star HD 18438

Byeong-Cheol Lee[1, 2, ⋆], **Jae-Rim Koo**[3], **Gwanghui Jeong**[1], **Myeong-Gu Park**[4], **Inwoo Han**[1], and **Yeon-Ho Choi**[1, 2]

[1]Korea Astronomy and Space Science Institute, 776, Daedeok-daero, Yuseong-gu, Daejeon, Republic of Korea
[2]Astronomy and Space Science Major, University of Science and Technology, 217, Gajeong-ro, Yuseong-gu, Daejeon, Republic of Korea
[3]Kongju National University, 56, Gongjudaehak-ro, Gongju-si, Chungcheongnam-do, Republic of Korea
[4]Department of Astronomy and Atmospheric Sciences, Kyungpook National University, 80, Daehak-ro, Buk-gu, Daegu, Republic of Korea
⋆Corresponding Author: B.-C. Lee, bclee@kasi.re.kr

Received July 26, 2021; Accepted March 15, 2023; Published March 20, 2023

Abstract

We have been conducting a exoplanet search survey using Bohyunsan Observatory Echelle Spectrograph (BOES) for the last 18 years. We present the detection of exoplanet candidate in orbit around HD 18438 from high-precision radial velocity (RV) mesurements. The target was already reported in 2018 (Bang et al. 2018). They conclude that the RV variations with a period of 719 days are likely to be caused by the pulsations because the Lomb-Scargle periodogram of *HIPPARCOS* photometric and H_α EW variations for HD 18438 show peaks with periods close to that of RV variations and there were no correlations between bisectors and RV measurements. However, the data were not sufficient to reach a firm conclusion. We obtained more RV data for four years. The longer time baseline yields a more accurate determination with a revised period of 803 $\pm$ 5 days and the planetary origin of RV variations with a minimum planetary companion mass of 21 $\pm$ 1 $M_{\rm Jup}$. Our current estimate of the stellar parameters for HD 18438 makes it currently the largest star with a planetary companion.

Keywords: star: individual: HD 18438 — techniques: radial velocities

1. Introduction

Until now, more than 4700 planets have been found in various stellar luminosity types. Specially, just ∼100 planets were detected in giant stars. Giants are likely to show more complex RV variations because of the direct effect of various surface processes on the line profiles: stellar pulsations, chromospheric activities, spots, and large convection cells.

In 2010, we started the Search for Exoplanet around Northern circumpolar Stars (SENS; Lee et al. 2015) at Bohyunsan Astronomical Observatory (BOAO). The main goal of the SENS is to observe stars that are accessible year round in order to have better sampling for our targets and thus increase the planet detection efficiency. From the SENS survey, we detected twenty planetary companions (Lee et al. 2015, 2017; Bang et al. 2018; Jeong et al. 2018; Lee et al. 2020) and several periodic RV variations, probably, due to processes other than orbital motions around G-, K-, and M-giant stars. Lack of knowledge about planet formation and evolution makes RV surveys of giant stars an important endeavor.

Bang et al. (2018; hereafter, TYB18) obtained precise RV measurements for HD 18438 using Bohyunsan Observatory Echelle Spectrograph (BOES; Kim et al. 2007) and found long-period radial velocity (RV) variations with period of 719.0 days. They concluded that the observed RV variations are likely to be caused by the pulsations because the Lomb-Scargle periodograms of *HIPPARCOS* photometric and H_α EW variations for HD 18438 show apparently non-negligible peaks at periods close to that of RV variations. However, at the time, a definite conclusion could not be reached due to the lack of data, uncertainty in verification, and the amplitude of the RV variation was at odds with typical Long Secondary Periods in giants.

In this paper, we present more robust detection of low-amplitude and long-period RV variations in HD 18438 with additional RV data obtained for four more years, possibly caused by a planetary companion. What the criteria for low amplitude and long-term RV variation mean is related to giants, generally based on periods below a km s^{-1} and over hundreds of days.

Table 1. RV measurements for HD 18438 from November 2010 to April 2021.

JD-2450000 (Days)	ΔRV ($m\,s^{-1}$)	$\pm\sigma$ ($m\,s^{-1}$)	JD-2450000 (Days)	ΔRV ($m\,s^{-1}$)	$\pm\sigma$ ($m\,s^{-1}$)	JD-2450000 (Days)	ΔRV ($m\,s^{-1}$)	$\pm\sigma$ ($m\,s^{-1}$)
5529.076993	−127.0	9.4	7378.110490	334.3	9.7	8863.099371	−93.3	11.3
5842.233812	−113.4	9.4	7401.925174	203.3	10.8	8932.000976	25.0	14.0
5933.100505	142.3	10.9	7414.948654	392.4	9.6	8933.018910	34.7	12.5
5962.981233	36.6	10.8	7423.943333	190.7	10.1	8942.949838	79.8	10.1
6259.127756	−321.8	9.7	7468.938303	271.1	9.6	8944.996838	151.4	12.2
6287.033915	−361.1	12.9	7490.997465	275.6	25.3	8969.977387	263.2	12.5
6288.154197	−373.9	10.1	7491.008796	232.1	11.6	9134.958971	153.0	11.1
6347.036601	−306.9	9.2	7527.980176	57.1	11.7	9134.971889	150.8	12.1
6551.230025	173.5	12.4	7528.978922	109.0	11.3	9149.294967	75.3	9.4
6578.267935	65.4	10.8	7529.966975	218.2	11.1	9149.306854	80.2	9.2
6616.998903	148.5	8.1	7530.976243	288.2	11.8	9150.025131	61.7	11.8
6714.059556	307.1	13.3	7672.942073	−60.9	14.0	9150.994632	38.6	8.3
6739.952656	200.3	11.2	7703.900322	−216.9	9.2	9161.069290	114.7	9.4
6808.051845	97.1	13.0	7705.102409	−184.4	8.0	9161.083075	120.0	10.9
6808.061359	93.3	15.0	7757.052180	−328.9	11.7	9162.182363	136.6	10.7
6808.068234	115.9	17.4	7758.076241	−359.1	9.2	9216.967993	−1.1	11.2
6922.125007	−175.0	13.3	7854.998117	−400.5	11.0	9218.049565	38.4	12.2
6964.052704	−393.2	11.9	8109.217336	115.3	10.6	9295.964472	−244.2	10.4
6965.262046	−468.8	9.3	8148.023617	310.7	10.9	9298.964320	−179.1	10.7
7094.000813	−236.0	14.3	8515.925612	−224.5	10.9	9302.005836	−167.3	16.7
7298.015438	−6.7	11.7	8830.219372	−129.4	10.1	9330.961200	−398.9	12.9
7330.115826	73.4	8.7	8862.014128	−99.9	8.7	—	—	—

In Section 2, we describe the observations and data reduction. In Section 3, the stellar characteristics of the host stars are derived. The orbital solutions of RV variation measurements are presented in Section 4. In Section 5, possible origins of RV variations were explained. Finally, we summarize the study in Section 6.

2. Observations and Reduction

The fiber-fed, high-resolution (R = 45000) BOES installed at the 1.8-m telescope of BOAO (Kim et al. 2007), Korea was used for all RV measurements. An iodine absorption (I_2) cell was used with a wavelength region of 4900−5900 Å. The average signal-to-noise (S/N) for the I_2 region was about 150 at typical exposure times ranging from 10 to 20 minutes.

In 2018, TYB18 reported the first result from seven years observations (from November 2010 to April 2017). We obtained additional spectra for the following four years (from December 2017 to April 2021). The IRAF software package was used for the basic reduction of spectra and precise RV measurements utilizing the I_2 cell were carried out with the RVI2CELL (Han et al. 2007) code, which is based on the method by Butler et al. (1996) and Valenti et al. (1995). To demonstrate a long-term RV stability, the RV standard star τ Ceti was observed. RVs measured by the BOES are constant with an rms scatter of ∼7 $m\,s^{-1}$ (Lee et al. 2013). In this paper, all data including the TYB18 paper were analyzed. The resultant RV measurements are listed in Table 1.

3. Stellar Characteristics

Fabricius et al. (2002) reported that giant HD 18438 is likely to be a binary system with an orbital separation of ∼1100 AU, including the main sequence star (TYC 4516-2148-1). Although the proper motion and parallax are almost the same and their masses are almost the same, it is still difficult to understand how they are related. Interestingly, however, a secondary mass (normalized to 1 AU) of 21.72 $M_{\rm Jup}{}^{+20.62}_{-19.84}$ was estimated around the giant HD 18438.

The main parameters for HD 18438 was acquired from the Gaia database (Gaia Collaboration et al. 2018; Kervella et al. 2019; Stassun et al. 2019) and the *HIPPARCOS* catalog (ESA 1997). Table 2 summarizes the basic stellar parameters.

4. Orbital Solutions of Radial Velocity Variations

In order to find the periodicity in the RV variations, we used the Generalized Lomb-Scargle periodogram (GLS; Zechmeister & Kürster 2009). Compared to the 'classical' Lomb-Scargle periodogram, it provides more accurate frequencies while less susceptible to aliasing. We combined all RV measurements by BOES into a single RV set, including 27 RVs taken over the last four years.

The resulting RV curve as a function of the time for HD 18438 is shown in Figure 1. The arrow in the figure denotes the time when we started to obtain additionally spectra after previously observed last point by TYB18. All the data were analyzed, yielding a bit different orbital solutions.

Table 2. Stellar parameters for HD 18438 and TYC 4516-2148-1

Parameter	Unit	HD 18438	TYC 4516-2148-1	Reference
Spectral type	—	M2.5 III	—	Abt (2008)
m_v	[mag]	5.49	—	*HIPPARCOS* (ESA 1997)
	[mag]	—	9.08	Fabricius et al. (2002)
B-V	[mag]	1.569 ± 0.015	—	van Leeuwen (2007)
age	[Gyr]	5.5 ± 2.4	—	This work
π	[mas]	4.443 ± 0.171	4.223 ± 0.035	Gaia Collaboration et al. (2018)
$T_{\rm eff}$	[K]	3860 ± 100	—	Gaia Collaboration et al. (2018)
	[K]	—	6164 ± 211	Stassun et al. (2019)
[Fe/H]	[dex]	-0.4 ± 0.1	—	Bang et al. (2018)
log g	[cgs]	0.9 ± 0.1	—	This work
	[cgs]	—	3.7 ± 0.1	Stassun et al. (2019)
$v_{\rm micro}$	[km s^{-1}]	2.7 ± 0.4	—	Bang et al. (2018)
$R_\star$	[$R_\odot$]	88.475 ± 4.424	—	Kervella et al. (2019)
	[$R_\odot$]	—	2.554 ± 0.182	Stassun et al. (2019)
$M_\star$	[$M_\odot$]	1.84 ± 0.09	—	Kervella et al. (2019)
	[$M_\odot$]	—	1.174 ± 0.184	Stassun et al. (2019)
$L_\star$	[$L_\odot$]	929 ± 41	7.558 ± 0.095	Gaia Collaboration et al. (2018)
$v_{\rm rot} \sin(i)$	[km s^{-1}]	5.5 ± 0.2	—	Bang et al. (2018)
$P_{\rm rot}/\sin(i)$	[days]	637	—	This work

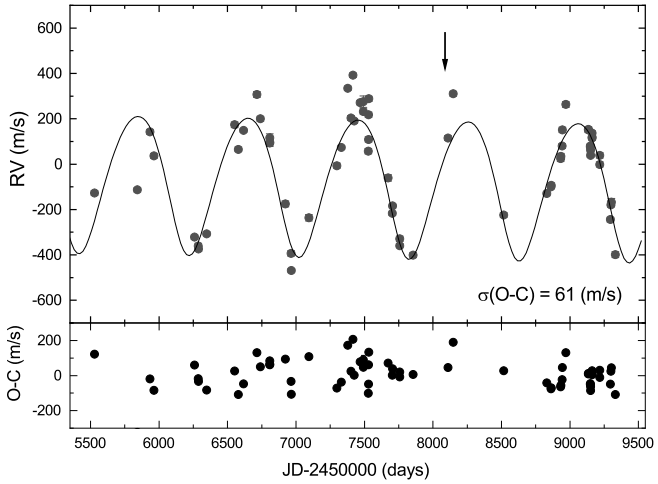

Figure 1. RV measurements (top panel) and the residuals (bottom panel) for HD 18438 from November 2010 to June 2021. The solid line is the orbital motion with a period of 803 days. The arrow marks April 2017, when we restarted to obtain more RV data.

Period changed from 719 to 803 days, semi-amplitude from 205 to 305 m s^{-1}, and an rms scatter (σ(O − C)) from 55 to 61 m s^{-1}. TYB18 reported two significant peaks at values of 719 days and ∼800 days in calculated RV periodogram in their Figure 5. They selected a relatively higher peak the last (719 days) as the main period. However, the whole RV set displays a unique peak with much increased confidence (top panel in Figure 2). Assuming a stellar mass of $1.84 \pm 0.09\ M_\odot$, minimum mass of the planetary companion is $21 \pm 1\ M_{\rm Jup}$ at a distance of 2.1 ± 0.1 AU from the host. A false alarm may appear in period analysis techniques when a period is incorrectly found where none exists in reality. Experimentally, FAPs below 0.01 (1%) mostly indicate a very secure period.

Table 3. Orbital parameters for HD 18438 b

Parameter	Unit	HD 18438
Period	[days]	803 ± 5
$T_{\rm periastron}$	[JD]	2455367 ± 45
K	[m s^{-1}]	305 ± 18
e	—	0.1 ± 0.1
ω	[deg]	167 ± 24
slope	[m s^{-1} day^{-1}]	-8.5×10^{-6}
Nobs	—	65
σ(O − C)	[m s^{-1}]	61
$m \sin(i)$	[$M_{\rm Jup}$]	21 ± 1.0
a	[AU]	2.1 ± 0.1

Keplerian orbital elements are listed in Table 3.

5. Origin of Radial Velocity Variations

Low-amplitude and long-term periodic RV variations in evolved stars may be caused by three kinds of phenomena: stellar pulsations, rotational modulations of surface features, or planetary companions. To find the origin of the RV variations observed in HD 18438, we have performed some validations that are currently possible: the *HIPPARCOS* photometry variations, the spectral line bisectors variations, and the stellar chromospheric activity variations. If one of these variations is similar to RV variations, it may invalidate the planetary companion interpretation.

5.1. Photometric Variations

In order to find feasible brightness variations caused by the rotational modulation of stellar spots or pulsations, we have

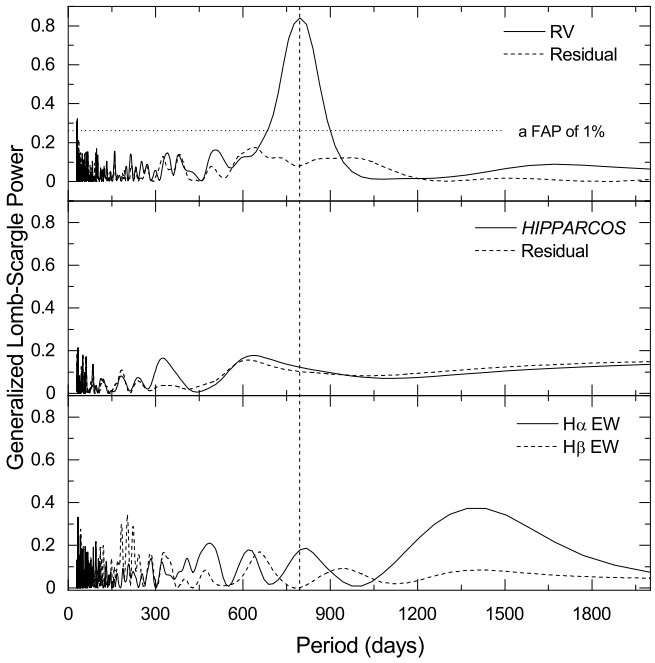

Figure 2. The GLS periodograms of the RV measurements, the *HIPPARCOS* photometry data, and the EW variations of the hydrogen lines (top to bottom panel) from 2010 to 2021. The vertical dashed line indicates the location of the period of 803 days. The solid line in the top panel is the GLS periodogram of the RV measurements for whole 11 years. The dashed line is the periodogram of the residual. The horizontal dotted line shows a FAP threshold of 1×10^{-2} (1%).

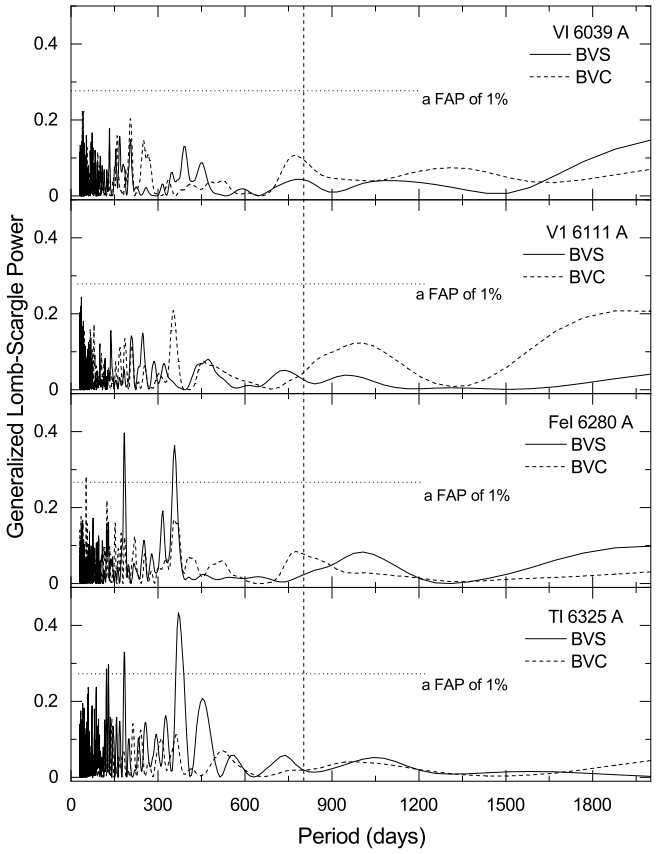

Figure 3. The GLS periodograms of the RV period and the four kinds of line bisectors for HD 18438. The horizontal dotted line shows a FAP threshold of 1×10^{-2} (1%) and the vertical dashed line indicates the location of the period of 803 days.

analyzed the *HIPPARCOS* photometric data which is the only relevant photometric data currently available. TYB18 shows a significant peak at about 700 days, close to 719 day RV period. In addition, there is another strong peak around 350 days, about a year, and it is half of period of a significant peak at about 700 days. However, we checked again using GLS or Lomb-Scargle periodograms and see no significant peaks at around 700 days or 350 days. In addition, no significant signal was found in the residual. (the middle panel in Figure 2).

5.2. Chromospheric Activities

The EW variations of Ca II H & K, H_α, H_β, sodium lines, and Ca II triplet lines are mostly used as chromospheric activity indicators, which are sensitive to the stellar atmospheric activity. Such activity could give a significant effect on the RV variations. However, our data do not have enough S/N ratio to resolve the emission feature in the Ca II H & K line cores. Ca II triplets are also not suitable because of fringing and saturations of our CCD spectra at wavelength longer than 8000 Å.

Thus, in this study we use the H_α and H_β lines. It is important to avoid nearby blending lines and weak telluric lines. We measured the H line EWs using a band pass of ±1.0 Å centered on the core of the H lines. The mean EWs of the H lines are measured to be 1138.4 ± 1.2 mÅ (H_α) and 934.5 ± 0.8 mÅ (H_β). The rms in the H_α and the H_β EWs correspond to under 0.1% variations. The GLS periodogram of the H line EW variations are shown in the bottom panel of Figure 2. There is no significant power at the frequency corresponding to the period around 783 days noted in TYB18.

TYB18 was failed to avoid nearby blending lines and weak telluric lines. That is, when a 2.0 Å band pass is specified, the EW change increases due to Co1 6563 Å around H_α line EW and Cr 4861 Å around H_β line EW. In this paper, the variation is less than 0.1% in H lines, however, with a band pass of 2.0 Å, the variation of ∼2% is calculated (See Figure 5 of Lee et al. 2012).

5.3. Line Bisector

Stellar rotational modulations of surface inhomogeneities can create variable asymmetries in the spectral line profiles (Queloz et al. 2001): the RV difference of the central values at high and low flux levels of the line profiles (BVS: bisector velocity span) and the difference of the velocity span of the upper half and lower half of the bisectors (BVC: the velocity curvature) (Hatzes et al. 2005; Lee et al. 2013). In order to calculate bisectors, we selected four unblended strong lines of V I 6039.7 Å, V I 6111.6 Å, Fe I 6280.6 Å, and Ti I 6325.2 Å that are located beyond the I_2 absorption region. To avoid the spectral core and wings, the BVS of the profile between two different flux levels at 0.8 and 0.4 of the central depth was used as the span points in the estimation. Figures 3 show the GLS periodograms of the each BVS and BVC for HD 18438. None of them show any meaningful periodic variations. Although

peaks are observed around ∼200 and ∼360 days, they are not found in photometric data or analysis of chromospheric activities, making it difficult to estimate a origin. Thus, long-term observations may be helpful to determine the exact cause of star with active surface activity.

6. Discussion

TYB18 found a long-period RV variation of 719 days in M2.5 giant HD 18438 and checked the *HIPPARCOS* photometry data, chromospheric activity, and bisectors in order to identify its origin. Of these, H_α EW and the *HIPPARCOS* photometric variations are close to that of RV variations of 719 days. They, thus, conclude that the RV variation may be caused by stellar pulsations.

We had four more years of observation since and revised the orbit solution for the whole data. The analysis of the RV measurements for HD 18438 revealed a new and clean period of 803 days, which is different from 719 days of TYB18. The H_α EW and H_β EW lines were used to monitor the chromospheric activities, which, however, do not reveal any significant evidence of variation. A study on the analysis of *HIPPARCOS* photometric data also does not show any meaningful variations nor the Bisectors reveal any relation with the RV measurements.

We also checked the variation of line broadening of the CCF(cross-correlation function), and its periodicity. As mentioned in Hatzes et al. (2018) and Delgado Mena et al. (2018), high luminosity giants such as γ Draconis and NGC 4349 No. 127 may have RV variations due to stellar activity and/or pulsation that cannot be detected by photometry, bisectors and chromospheric lines and can be detected by CCF. However, we did not find any long-period variation on the CCF obtained from BOES data. We thus concluded that there are no low-amplitude Long-Sencondary Periods (LSP; Wood et al. 2004) related to dipole oscillating convection modes. Although such long period pulsation may be associated with LSP, typical amplitude of RV variations in LSP is much larger that in HD 18438.

Rotation period (upper limit) of 562 days is also too short to explain the observed RV period. All the evidence has now convinced us that there is a planetary companion. We conclude that M2.5 giant HD 18438 host a planetary companion with a minimum mass of 21 $M_{\rm Jup}$. This value is almost consistent with the secondary mass combination estimated by Stassun et al. (2019).

The residual RV variations (61 m s^{-1}) after orbital fitting do not show any additional periodic signal as shown in the top panel of Figure 2. The scatters are considerably greater than the RV precision the RV standard star τ Ceti (7 m s^{-1}) and the individual RV accuracies from our survey of ∼12 m s^{-1}. The rms of K giant RV residuals has a typical value of 20 m s^{-1} (Hekker et al. 2006), which increases toward later spectral type. Lee et al. (2013) have shown larger residuals from M giants, ∼39 m s^{-1} in M1 giant HD 208527 and ∼57 m s^{-1} in M2 giant HD 220074.

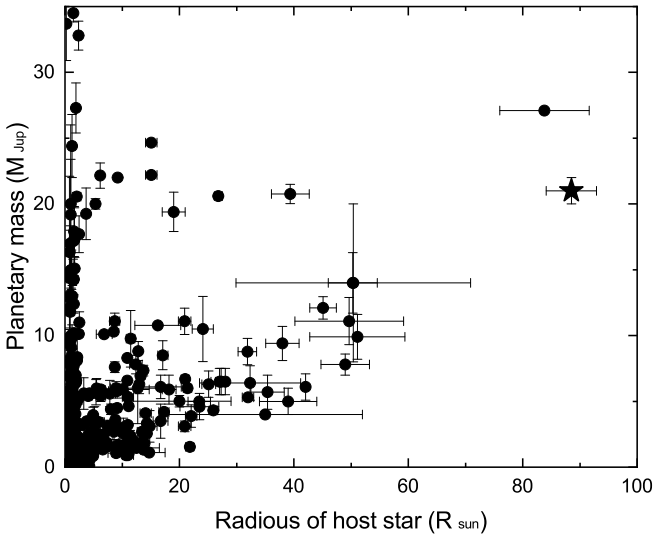

Figure 4. Distribution of stellar radii vs. minimum masses of planetary companions as of July 2021. Pentagram denotes the planetary companion around HD 18438.

Figure 4 shows the distribution of currently confirmed exoplanets from The Extrasolar Planets Encyclopaedia archive[1] in the diagram for the radius of host stars versus the mass of planetary companions. Of the ∼4700 host stars harboring planetary companions with known stellar radii, more 95% are smaller than 5 $R_\odot$ (∼0.025 AU). The pentagram at $R_\star$ = 88 $R_\odot$ in Figure 4 is HD 18438, which will be at the moment, the largest star with a planetary companion. The rightmost star is HD 81817, which is the largest star and happens to be a hybrid star, with a brown dwarf candidate (Bang et al. 2020).

The fate of planets changes dramatically as it evolves from the MS stage to the evolved stage, such as the red giant branch (RGB) and the asymptotic giant branch (AGB). The companions may be engulfed or moved outward by the expanding star when the latter increases its radius as it evolves. Considering its luminosity and temperature, HD 18438 is located at the AGB stage on the H–R diagram after undergoing the helium flash. It is still unknown what happens to the companion when it interacts with the atmosphere of expanding host star. Discovery and study of highly evolved planetary systems such as HD 18438 will help understand the late and final fates of the planetary systems.

Acknowledgments

B.C.L acknowledges partial support by the KASI (Korea Astronomy and Space Science Institute) grant 2021-1-830-08 and acknowledge support by the National Research Foundation of Korea (NRF) grant funded by the Korea government (MSIT) (No. 2021283200). M.G.P. was supported by the Basic Science Research Program through the National Research Foundation of Korea (NRF) funded by the Ministry of Education (2019R1I1A3A02062242) and KASI under the R&D program supervised by the Ministry of Science, ICT and Future

[1] http://exoplanet.eu/

Planning. This research made use of the SIMBAD database, operated at the CDS, Strasbourg, France.

References

Abt, H. A. 2008, ApJS, 176, 216
Bang, T.-Y., Lee, B.-C., Jeong, G.-h., Han, I., & Park, M.-G. 2018, JKAS, 51, 17
Bang, T.-Y., Lee, B.-C., Perdelwitz, V., et al. 2020, A&A, 638, A148
Butler, R. P., Marcy, G. W., Williams, E., et al. 1996, PASP, 108, 500
Delgado Mena, E., Lovis, C., Santos, N. C., et al. 2018, A&A, 619, A2
ESA. 1997, The HIPPARCOS and TYCHO catalogues, ESA SP-1200
Fabricius, C., Høg, E., Makarov, V. V., et al. 2002, A&A, 384, 180
Gaia Collaboration, Brown, A. G. A., Vallenari, A., et al. 2018, A&A, 616, A1
Han, I., Kim, K.-M., Byeong-Cheol, L., & Valyavin, G. 2007, Publication of the Korean Astronomical Society, 22, 75
Hatzes, A. P., Guenther, E. W., Endl, M., et al. 2005, A&A, 437, 743
Hatzes, A. P., Endl, M., Cochran, W. D., et al. 2018, AJ, 155, 120
Hekker, S., Reffert, S., Quirrenbach, A., et al. 2006, A&A, 454, 943
Jeong, G., Han, I., Park, M.-G., et al. 2018, AJ, 156, 64
Kervella, P., Arenou, F., Mignard, F., & Thévenin, F. 2019, A&A, 623, A72
Kim, K.-M., Han, I., Valyavin, G. G., et al. 2007, PASP, 119, 1052
Lee, B. C., Han, I., & Park, M. G. 2013, A&A, 549, A2
Lee, B. C., Mkrtichian, D. E., Han, I., Park, M. G., & Kim, K. M. 2012, A&A, 548, A118
Lee, B.-C., Park, M.-G., Han, I., et al. 2020, JKAS, 53, 27
Lee, B. C., Park, M. G., Lee, S. M., et al. 2015, A&A, 584, A79
Lee, B.-C., Jeong, G., Park, M.-G., et al. 2017, ApJ, 844, 36
Queloz, D., Henry, G. W., Sivan, J. P., et al. 2001, A&A, 379, 279
Stassun, K. G., Oelkers, R. J., Paegert, M., et al. 2019, AJ, 158, 138
Valenti, J. A., Butler, R. P., & Marcy, G. W. 1995, PASP, 107, 966
Wood, P. R., Olivier, E. A., & Kawaler, S. D. 2004, ApJ, 604, 800
Zechmeister, M., & Kürster, M. 2009, A&A, 496, 577